

# IL-17 induces macrophages to M2-like phenotype via NF- $\kappa$ B

Jing Shen<sup>1,\*</sup>  
 Xin Sun<sup>2,\*</sup>  
 Bo Pan<sup>1</sup>  
 Shoubo Cao<sup>1</sup>  
 Jingyan Cao<sup>1</sup>  
 Dehai Che<sup>1</sup>  
 Fang Liu<sup>1</sup>  
 Shuai Zhang<sup>1</sup>  
 Yan Yu<sup>1</sup>

<sup>1</sup>Department of Medical Oncology, Harbin Medical University Cancer Hospital, Harbin, People's Republic of China; <sup>2</sup>Department of Cardiology, The First Affiliated Hospital, Cardiovascular Institute, Harbin Medical University, Harbin, People's Republic of China

\*These authors contributed equally to this work

**Background:** Tumor-associated macrophage (TAM) is emerging as one of the important complications in cancer promotion. Interleukin-17 (IL-17), a potent pro-inflammatory cytokine, plays an active role in promoting M2 macrophage differentiation (TAMs are M2-like phenotypes). In this study, we aimed to evaluate that IL-17 stimulates key phenotypic and functional signatures of M2 macrophages associated with cancer progression in non-small-cell lung cancer (NSCLC) patients.

**Patients and methods:** The markers and cytokines of M2 macrophages were detected in THP-1-derived macrophages and mouse peritoneal macrophages treated with IL-17. The activation of nuclear factor kappa B (NF- $\kappa$ B) and nuclear localization of p65 in IL-17-treated cells were investigated. The BAY11-7082 inhibitor and the siRNA of p65 were used to block the NF- $\kappa$ B activation. A total of 85 patients who underwent surgery for histologically verified NSCLC were enrolled in this study. The expression of IL-17 and M2 macrophage markers were assessed by immunostaining. Survivals were estimated using the Kaplan–Meier method.

**Results:** The CD163 and CD206 cell surface markers and transforming growth factor beta (TGF- $\beta$ ), vascular endothelial growth factor (VEGF) and IL-10 of M2 macrophages were significantly increased in IL-17-treated THP-1-derived macrophages in a dose-dependent manner. IL-17 increased the mRNA levels of Arginase I and Fizz1, the phosphorylation of I $\kappa$ B $\alpha$  and nuclear localization of p65 (a subunit of NF- $\kappa$ B). The BAY11-7082 abrogated IL-17-induced CD206 and CD163 expression, TGF- $\beta$ , VEGF, IL-10, Arginase I and Fizz1 expression and p65 nuclear translocation. Further experiments showed that IL-17 induced the expression of CD206, CD163, Arginase I, Fizz1 and Ym1 in mouse peritoneal macrophages that were inhibited by siRNA of p65. The immunostaining experiments on human NSCLC tissues indicated that high IL-17 expression was significantly correlated with CD163 and c-Maf. The intratumoral IL-17+ CD163+ c-Maf+ cells were associated with NSCLC progression.

**Conclusion:** IL-17 stimulated macrophages to M2-like phenotypes via NF- $\kappa$ B activation. IL-17 may be a potential therapeutic target for NSCLC.

**Keywords:** IL-17, M2 macrophages, NF- $\kappa$ B, non-small-cell lung cancer, survival

## Introduction

The tumor microenvironment comprises various tumor cells, stromal cells, extracellular matrix and cytokines, playing an important role in tumor progression and metastasis.<sup>1</sup> Macrophages are the dominant migratory leukocyte population found in the tumor microenvironment. Tumor-associated macrophages (TAMs) are correlated with poor prognosis in several types of cancers including non-small-cell lung cancer (NSCLC).<sup>2</sup> Macrophages are differentiated from circulating bone marrow-derived

Correspondence: Yan Yu  
 Department of Medical Oncology, Harbin Medical University Cancer Hospital,  
 No 150 Haping Road, Harbin 150081,  
 People's Republic of China  
 Tel/fax +86 451 8629 8727  
 Email yuyan@ems.hrbmu.edu.cn

monocytes with widely different properties depending on the external criteria. Macrophages are also highly plastic and can rapidly alter their phenotype as local signals change. The macrophages at the two extremes of possible differentiation states are the classically activated type 1 (M1) and the alternatively activated type 2 (M2).<sup>3</sup> M1 macrophages are polarized by lipopolysaccharide (LPS), certain Toll-like receptor (TLR) agonism, tumor necrosis factor  $\alpha$  (TNF $\alpha$ ), interferon- $\gamma$  and mediate the innate immunity.<sup>3,4</sup> M1 macrophages are well adapted to express high levels of inducible nitric oxide synthase (iNOS), reactive oxygen species (ROS), TNF $\alpha$ , interleukin (IL)-1 $\beta$ , IL-6, IL-12, IL-18, IL-23, CXCL10, human leukocyte antigen-DR and nitrogen intermediates. The macrophages that are exposed to Th2 cells and tumor-derived cytokines such as IL-4, IL-10, IL-13, transforming growth factor beta (TGF- $\beta$ ) or prostaglandin E2 (PGE2) promote M2 polarization.<sup>5</sup> M2 macrophages secrete vascular endothelial growth factor (VEGF), Arginase I, Ym1 (chitinase 3-like 3, also known as Ym1), Fizz1 (resistin-like beta, also known as Fizz1) and cytokines such as IL-1ra, decoy IL-1RII, IL-10, CCL17, CCL18, CCL22, polyamine, scavenger R and mannose R. M2 macrophages are associated with immunoregulation, tissue remodeling, tumor growth promotion and metastasis.<sup>6</sup> Common cell surface targets identified to separate M2 macrophage subsets include CD204, CD163, CD206 and CD301.<sup>7</sup> Meanwhile, no unique cell surface marker has yet been identified for M1 macrophages.

It has been broadly characterized that TAMs are M2-like phenotypes.<sup>8</sup> Over the years, significant efforts have been focused on exploiting the properties of TAMs within the tumor microenvironment.<sup>9</sup> NSCLC patients with high TAM density are correlated with poor survival, suggesting that TAMs are significant factors of NSCLC prognosis.<sup>10</sup> The cytokines expressed by TAMs can influence the tumor microenvironment and develop neoplasias and promote tumor cell migration and invasion.

IL-17 is a pleiotropic cytokine that plays a vital role in many chronic inflammatory diseases, autoimmune diseases, tumors and in host defense against bacterial and fungal infections.<sup>11</sup> Although it was originally considered that IL-17 was produced by T-helper cell subset, TH17 cells, recent studies showed that a wide range of innate immune cells, including  $\gamma\delta$ T cells, lymphoid tissue inducer (LTi) cells, invariant natural killer T (iNKT) cells, natural killer (NK) cells and neutrophils, are also considerable sources of its early production.<sup>12</sup> IL-17 can promote recruitment of macrophages and induce their cytokine/chemokine production, mediating a

link between acquired and innate immunity,<sup>13</sup> specifically T-cell and macrophage functions.<sup>14</sup> It has been reported that IL-17-mediated inflammation related to M1/M2 macrophage alterations induced by zoledronate may be beneficial for cancer therapy and that blocking IL-17 activity significantly decreased the M1/M2 ratio.<sup>15</sup> However, very little is known about the mechanism through which IL-17 mediates the polarization of macrophages. Recent studies showed that IL-17 stimulated the phosphorylation of nuclear factor kappa B inhibitor alpha (I $\kappa$ B $\alpha$ ), suggesting the activation of the nuclear factor kappa B (NF- $\kappa$ B) signaling pathway.<sup>16,17</sup> Thus, in this study, we aimed to elucidate the exact role and associated molecular mechanism of IL-17 in macrophage polarization.

In this study, we verified that IL-17 stimulated macrophages to M2-like phenotype via the NF- $\kappa$ B signaling pathway and that the high density of M2 macrophages was correlated with poor survival in NSCLC patients.

## Patients and methods

### Patients

A total of 85 patients who underwent surgery with pathologically confirmed NSCLC at the Department of Pathology, Harbin Medical University Cancer Hospital, between 2006 and 2010 were enrolled in this study. No patients received any anti-tumor therapy prior to sample collection. The tumor stage was determined according to the 2010 American Joint Committee on Cancer and International Union Against Cancer tumor-node-metastasis (TNM) classification system. Tumor differentiation was graded according to the Edmondson and Steiner grading system. All experiments were performed in accordance with the relevant guidelines and regulations of Harbin Medical University. This study was approved by the ethics committee of Harbin Medical University, and written informed consent was obtained from each patient.

### Cell culture and treatment

A human leukemic cell line, THP-1 cell (American Type Culture Collection, Manassas, VA, USA), was cultured in RPMI 1640 medium containing 10% fetal bovine serum, 20  $\mu$ g/mL penicillin and 20  $\mu$ g/mL streptomycin at 37°C in a humidified atmosphere with 5% CO<sub>2</sub>. The cells were differentiated into macrophages by adding 50 ng/mL of phorbol-12-myristate-13-acetate (PMA; EMD Biosciences, La Jolla, CA, USA) for 48 hours in 35 mm Petri dishes. After differentiation, THP-1 cells were, respectively, treated with 10, 20, 50 and 100 ng/mL of recombinant human IL-17 (R&D Systems, Inc., Minneapolis, MN, USA) for 48 hours. Then, the THP-1 cells were

treated with 100 ng/mL of recombinant human IL-17 for 0, 24 and 48 hours, respectively. To inhibit NF- $\kappa$ B pathways, the cells were incubated with 10 mM BAY11-7082 (Beyotime Institute of Biotechnology, Jiangsu, China) accompanied by IL-17 for 48 hours.

## Flow cytometry

Cells ( $1 \times 10^5$  cells per 100  $\mu$ L) were washed with PBS 0.2% Tween-20 for four times and then centrifuged at  $400 \times g$  for 5 minutes. Cells were blocked with 5% BSA for 30 minutes, washed for four times, incubated with fluorescein isothiocyanate (FITC)-CD206 mAb (BD Biosciences, San Jose, CA, USA), anti-CD11b antibody [44aacb] (FITC) (Abcam, Cambridge, UK) and anti-F4/80 antibody [CI:A3-1] (phycoerythrin) (Abcam) for 45 minutes at 4°C in the dark. Following the final washing step, labeled cells were resuspended to 500  $\mu$ L in PBS, 10% fetal calf serum and analyzed by flow cytometry on a FACScan flow cytometer using Cell Quest software (BD Biosciences).

## Transient transfection with siRNA

siRNA-p65 and negative control RNA molecules with mismatched sequences were synthesized by Oligofectamine (Thermo Fisher Scientific, Waltham, MA, USA) using the following sense and anti-sense strands: siRNA-p65-1 sense, 5'-CAAGGUGCAGAAAGA-3' and antisense, 5'-UCUUUCUGCACCUUGUCGC-3'; siRNA-p65-2 sense, 5'-GUUUCAGCAGCUCCUGAACTT-3' and antisense, 5'-GUUCAGGAGCUGCUGAACTC-3' and scramble siRNA sense, 5'-TTCAAGUCCUCGACGACUUUG-3' and antisense 5'-CTCAAAGUCGUCGAGUUUG-3', and transfection into mouse peritoneal macrophages cells was

performed using Lipofectamine™ 2000 (Thermo Fisher Scientific) according to the manufacturer's instructions.

## Real-time qRT-PCR analysis

Total RNA was extracted using the Trizol reagent (Thermo Fisher Scientific) according to the manufacturer's protocol. Complementary DNA was synthesized from 500 ng of total RNA using the PrimeScript™ RT reagent kit with DNA Eraser (Takara Bio, Inc, Dalian, China). Semiquantitative real-time PCR was performed using the SYBR Green Master Mix (Hoffman-La Roche Ltd., Basel, Switzerland) on an ABI7500 Sequence Detection System (Thermo Fisher Scientific). Glyceraldehyde 3-phosphate dehydrogenase (GAPDH) was used as the internal control to correct for variations in the cDNA content among the samples. The primers were synthesized by Oligofectamine (Takara Bio, Inc) (Table 1). No amplification of nonspecific products was observed in any of the reactions, as determined from an analysis of the dissociation curves.

## Western blot analysis

Total protein extracts were prepared from cells by homogenization in lysis buffer containing protease inhibitor cocktail (Complete; Hoffman-La Roche Ltd.) and phosphatase inhibitor (Hoffman-La Roche Ltd.). The membrane was then incubated with primary antibody against p-I $\kappa$ B $\alpha$  (1:200; Cell Signaling Technology, Danvers, MA, USA), I $\kappa$ B $\alpha$  (1:1,000; Beyotime Institute of Biotechnology),  $\beta$ -actin (1:500; Beyotime Institute of Biotechnology), p65 (1:500; Beyotime Institute of Biotechnology), GAPDH (1:2,000; Beyotime Institute of Biotechnology) and Lamin B (1:1,000; Cell Signaling Technology) in the same solution overnight at 4°C. The blot was rinsed and

**Table 1** Primers for real-time PCR

	Forward (5'-3')	Reverse (5'-3')
<b>Human</b>		
TGF- $\beta$	GATGTCACCGGAGTTGTGC	TGCAGTGTGTTATCCCCTGCT
IL-6	TACATCCTCGACGGCATCTC	CCATCTTTGGAAGGTTCCAGG
Fizz1	GCAAGAAGCTCTCGTGTGCTAGTG	CGAACCACAGCCATAGCCACAAG
Arginase I	CACACCAGCTACTGGCACACC	GCAACTGCTGTGTTCACTGTTCG
VEGF	TCCTCACACCATTGAAACCA	ATCCTGCCCTGTCTCTCTGT
IL-10	CCAAGACCCAGACATCAAGG	AAGGCATTCTTCACCTGCTC
GAPDH	AGAAGGCTGGGGCTCATTG	AGGGGCCATCCACAGTCTTC
<b>Mouse</b>		
p65	GGTAGCCAAACAGGA	GAAGAGGGAAGAAGC
Fizz1	CTTGTGGCTTTGCCGTGTGGA	GCAGTGGTCCAGTCAACGAG
Arginase I	TGCTCACACTGACATCAACTCC	TCTACGTCTCGAAGCCAAATGTAC
Ym1	GAATGAAGGAGCCACTGAGGTCTG	TTGTTGTCCTTGAGCCACTGAGC
GAPDH	GAGGACCAGTTGTCTCTCTG	GGATGGAATTGTGAGGGAGA

**Abbreviations:** GAPDH, glyceraldehyde 3-phosphate dehydrogenase; IL, interleukin; TGF- $\beta$ , transforming growth factor beta; VEGF, vascular endothelial growth factor.

incubated with HRP-conjugated secondary antibody (1:2,000; Zhongshan Golden Bridge Biotechnology Co., Beijing, China) at 37°C for 1 hour. Protein bands were visualized using an ECL kit (Transgen Biotechnology Co. Ltd., Beijing, China) and captured with a scanner (Epson V30, Seiko Epson Corporation, Tokyo, Japan). Data were quantified using Quantity One Version 4.6.2 (Bio-Rad Laboratories Inc., Hercules, CA, USA).

### iNOS activity assay

Cellular iNOS activity was measured by the conversion of L-arginine to NO by the use of a nitric oxide synthase assay kit (Beyotime Institute of Biotechnology).

### Immunofluorescence staining and ELISA

For immunofluorescence staining, cells were fixed with 4% paraformaldehyde for 15 minutes at room temperature and permeabilized by treating with 100% methanol for 10 minutes at 20°C. Then, the slides were washed with PBS, blocked with normal goat IgG for 1 hour at room temperature and incubated overnight at 4°C with rabbit anti-NF- $\kappa$ B p65 antibodies (1:200; Beyotime Institute of Biotechnology) or rabbit anti-CD163 antibodies (1:100; Boster Biological Technology, Wuhan, China). Then, the slides were rinsed twice in PBS and incubated with FITC-conjugated anti-rabbit antibody (Zhongshan Golden Bridge Biotechnology) or tetramethylrhodamine-5-isothiocyanate-conjugated anti-rabbit antibody (Zhongshan Golden Bridge Biotechnology) diluted 1:100 at 37°C for 1 hour. Slides were then mounted with Prolong Gold Antifade Reagent with 4',6-diamidino-2-phenylindole (DAPI; Thermo Fisher Scientific). The fluorescent images were analyzed by fluorescence microscopy.

Angiogenic factor concentrations were determined using a commercial ELISA kit (Uscn Life Science, Houston, TX, USA) according to the manufacturer's instructions.

### Immunohistochemistry staining

Immunohistochemistry staining was performed as previously described.<sup>18</sup> The primary antibodies and dilutions were as follows: anti-IL-17 antibody (1:100; Santa Cruz Biotechnology Inc., Dallas, TX, USA), anti-CD163 antibody (1:100; Boster) and anti-cellular homologue of avian musculoaponeurotic fibrosarcoma virus oncogene (c-Maf) antibody (Abcam). The negative control sections were treated with PBS instead of the primary antibodies.

Stained tissue sections were evaluated using light microscopy at 200 $\times$  or 400 $\times$  magnification by two pathologists. Five representative fields of each case were captured. To calculate

the percentages of IL-17- and CD163-positive cells, the number of positive-staining cells and total number of cells in five count areas of each photograph were measured using Image-Pro Plus v6.0 software (Media Cybernetics, Inc., Silver Spring, MD, USA). The mean percentage of positive cells was calculated as the quotient of the number of positive cells divided by the total number of cells.

### Statistics

Statistical analysis was performed with SPSS 17.0 software (SPSS, Chicago, IL, USA). Each treatment was performed in duplicate, and the experiment was independently repeated three times. Measurement values were expressed as mean $\pm$ SD. One-way analysis of variance followed by the Student–Newman–Keuls test and Spearman's  $r$  correlation were used as appropriate. The survival rates were calculated by the Kaplan–Meier method (log-rank test). Cox multivariate analysis with a stepwise method (forward, likelihood ratio) was used to determine the independent prognostic factors. A  $P$  value of  $<0.05$  was judged to indicate significant results. The median values of the percentage of IL-17+ cells and of CD 163+ cells were used as cutoffs to dichotomize the immunostaining.

## Results

### IL-17 promotes M2 macrophage differentiation in a concentration-dependent manner

To characterize the effect of IL-17 on polarized THP-1-derived macrophages to M2 phenotype, the THP-1-derived macrophages were treated with IL-17 at 0, 10, 50 and 100 ng/mL for 48 hours. The CD206 cell surface marker of M2 macrophages was significantly increased in IL-17-treated THP-1-derived macrophages in a dose-dependent manner compared to control cultures (0 ng/mL as PBS) (Figure 1A). Chemokines, cytokines and enzymes linked to subset-specific functions have helped to distinguish the macrophage phenotypes.<sup>19</sup> The cytokines expressed by the two subsets of macrophages were measured. We found that TGF- $\beta$ , VEGF and IL-10 for M2 macrophage were produced in the IL-17-cultured medium significantly more than in control, while there was no significant difference in IL-6 for M1 macrophage (Figure 1B). We observed a more significant increase in mRNA levels (Figure 1C). The level of iNOS can be combined with the cytokines for more accurate identification of M1 macrophage.<sup>19</sup> After being treated with IL-17, the level of iNOS revealed no statistical difference (Figure 1D).

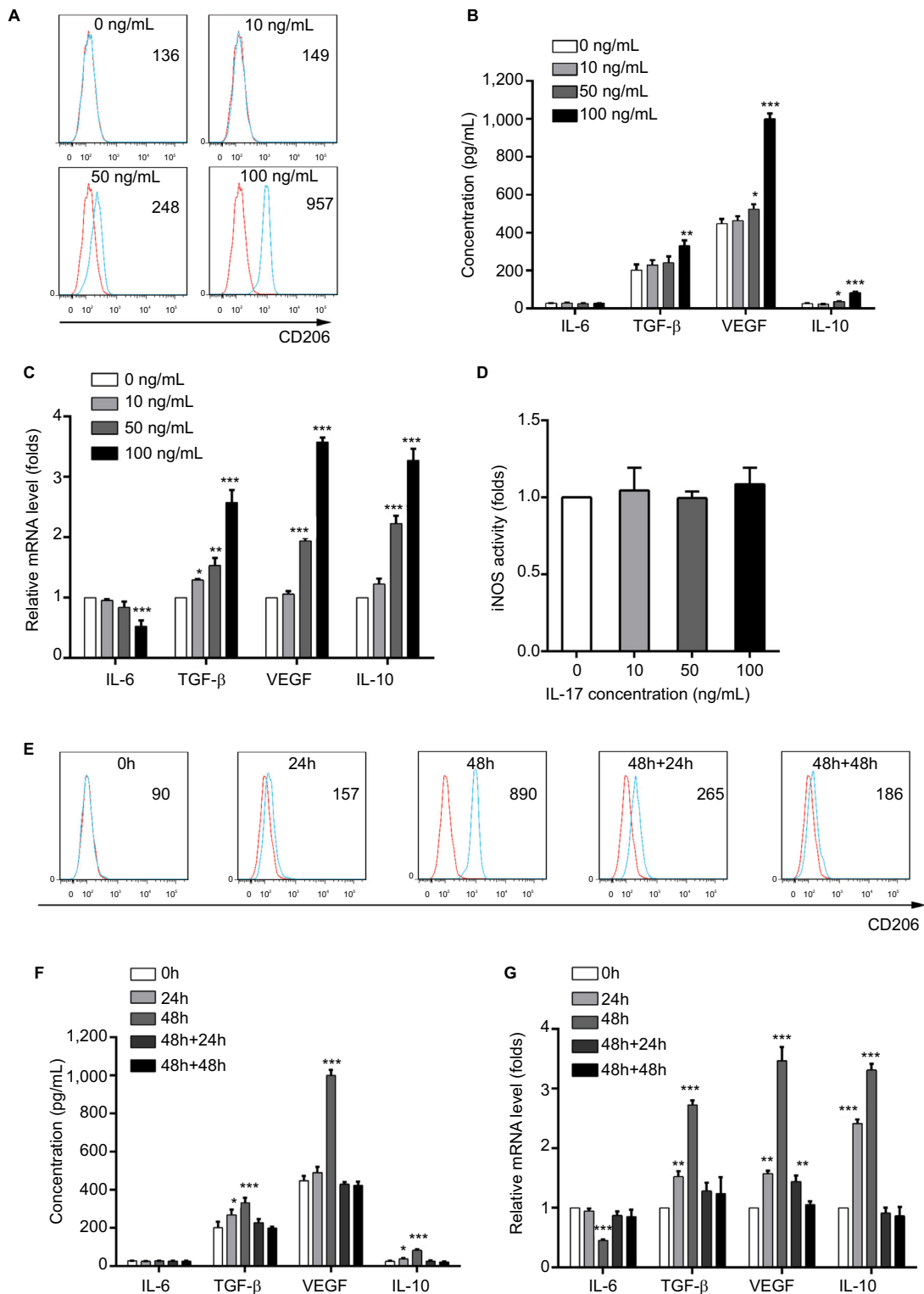


**Figure 1** IL-17 induces M2-like phenotype in THP-1-derived macrophages.

**Notes:** (A) THP-1-derived macrophages were treated with IL-17 at 0, 10, 50 and 100 ng/mL for 48 hours. The expression of CD206 was detected by flow cytometry. The histograms are representatives of three independent experiments. Numerical values denote the mean fluorescence intensity. The red line is the fluorescence intensity of isotype control. The blue line is the fluorescence intensity of CD206. (B) ELISA analysis of cytokine levels in the media of IL-17-treated THP-1-derived macrophages. The data shown represent mean±SD (n=3 per group, \*P<0.05, \*\*P<0.01 and \*\*\*P<0.001). (C) qRT-PCR of TGF-β, VEGF, IL-10 and IL-6 mRNA levels. Relative expression was obtained using the 2<sup>-ΔΔCt</sup> method after normalization to GAPDH. Histogram shows mean±SD of mRNA expression in three separate experiments (n=3 per group, \*P<0.05, \*\*P<0.01 and \*\*\*P<0.001). (D) iNOS activity was measured. The data shown represent mean±SD (n=3 per group). (E) Cells were stained with CD206 antibody. Numerical values denote the mean fluorescence intensity. The red line is the fluorescence intensity of isotype control. The blue line is the fluorescence intensity of CD206. (F) ELISA-determined cytokine levels were expressed as mean±SD (n=3 per group, \*P<0.05 and \*\*\*P<0.001). (G) qRT-PCR of TGF-β, VEGF, IL-10 and IL-6 mRNA levels. The data shown represent mean±SD (n=3 per group, \*\*P<0.01 and \*\*\*P<0.001).

**Abbreviations:** GAPDH, glyceraldehyde 3-phosphate dehydrogenase; h, hour; IL, interleukin; iNOS, inducible nitric oxide synthase; qRT-PCR, quantitative real-time PCR; TGF-β, transforming growth factor beta; VEGF, vascular endothelial growth factor.



These findings demonstrated that IL-17 plays a potential role in promoting THP-1-derived macrophages to a M2-like phenotype in a dose-dependent manner.

### THP-1-derived macrophages polarized to M2 phenotype require sustained IL-17 treatment

To further dissect the functional roles of IL-17 in promoting THP-1-derived macrophages to a M2-like phenotype, we cultured the THP-1-derived macrophages in culture medium with 100 ng/mL of IL-17 for 48 hours and then cultured without IL-17 for 24 hours (48h+24h) or 48 hours (48h+48h). The CD206 was detected by flow cytometry analysis, which was significantly induced after IL-17 treatment, but this effect was eliminated by removing IL-17 (Figure 1E). The cytokines TGF- $\beta$ , VEGF and IL-10 for M2 macrophage were increased with increase in time, but after the absence of IL-17 the expression of the cytokines was decreased (Figure 1F and G). We demonstrated that the activation of M2-like phenotype was time dependent, increasing significantly after 24 hours of IL-17 stimulation and reaching maximal level at 48 hours. These results indicate that IL-17 is necessary for THP-1-derived macrophages to induce macrophage activation to a M2-like phenotype.

### IL-17 induces THP-1-derived macrophages to a M2-like phenotype via NF- $\kappa$ B

Some studies have previously shown that IL-17 activates NF- $\kappa$ B.<sup>20,21</sup> Thus, we thought to determine whether the M2 polarization observed in THP-1-derived macrophages under IL-17 conditions was attributable to increased NF- $\kappa$ B activity. THP-1-derived macrophages were incubated with IL-17 for 48 hours; we observed increased CD163 and CD206 levels, as determined by immunofluorescence staining and flow cytometry analysis (Figures 2A and 3). Immunoblotting with a specific antibody against p-I $\kappa$ B $\alpha$  was performed to detect the phosphorylation of I $\kappa$ B $\alpha$  and activation of NF- $\kappa$ B after IL-17 treatment. IL-17 stimulated increased phosphorylation of I $\kappa$ B $\alpha$  (Figure 2B), suggesting that the NF- $\kappa$ B pathway was activated in the IL-17-treated cells.

We investigated the potential for inhibition of NF- $\kappa$ B to attenuate the M2-like phenotype characteristics of IL-17-treated THP-1-derived macrophages. We used a commercially available IKK inhibitor, BAY11-7082, to pharmacologically block NF- $\kappa$ B activity in these cells. The BAY11-7082 inhibitor dramatically inhibited IL-17-induced

expression of CD163 and CD206 and phosphorylation of I $\kappa$ B $\alpha$  (Figures 2A and 3). IL-17 induced p65 nuclear translocation, which was inhibited by BAY11-7082 (Figure 2C and D). We found that IL-17-induced expression of TGF- $\beta$ , VEGF and IL-10 was inhibited by BAY11-7082 (Figure 2E), but there was no statistical difference in iNOS (Figure 2G). The mRNA levels of Arginase I and Fizz1 were examined in THP-1-derived macrophages. Compared with control cells, mRNA levels of Arginase I and Fizz1 were significantly increased in IL-17-treated cells. BAY11-7082 abrogated IL-17-induced increase in Arginase I and Fizz1 mRNA levels (Figure 2F).

### IL-17 induces CD203 and CD163 expression in mouse peritoneal macrophages via p65

The mouse peritoneal macrophages were cultured with 100 ng/mL of IL-17 for 48 hours and exposed to p65 siRNA (siRNA-p65-1/2) or empty vector. The isolated mouse peritoneal cells were authenticated by F4/80 and CD11b antibodies. There were 82.2% of macrophages in the isolated mouse peritoneal cells (Figure 4A). The level of protein and mRNA of p65 was decreased by siRNA-p65-1 and siRNA-p65-2 (Figure 4B and C). The levels of CD206 and CD163 were increased by IL-17, but the increase was inhibited in siRNA-p65-2 cells (Figure 4D–F). Compared with control cells, the mRNA levels of Arginase I, Fizz1 and Ym1 were significantly increased in IL-17-treated cells, but siRNA-p65-2 abrogated IL-17-induced increase in the mRNA levels of Arginase I, Fizz1 and Ym1 (Figure 4G).

### CD163 and c-Maf expression positively correlates with IL-17+ cell and predicts poor survival of NSCLC patients

To determine whether our findings are clinically relevant, we examined 85 NSCLC cases from the Harbin Medical University Cancer Hospital for the expression of CD163, c-Maf and IL-17. The immunostained tissue sections revealed more IL-17+ cells in cancers with high CD163 and c-Maf expression than in cancers with low IL-17 expression (Figure 5A). We found that the percentage of IL-17+ cells was positively correlated with the percentage of CD163+ c-Maf+ cells (Figure 5B).

We next investigated the prognostic value of IL-17, CD163 and c-Maf in NSCLC patients. The median survival time was 36.0 months (95% CI, 24.255–47.745) for all cases, and 17 patients were still alive at present. The survival rate

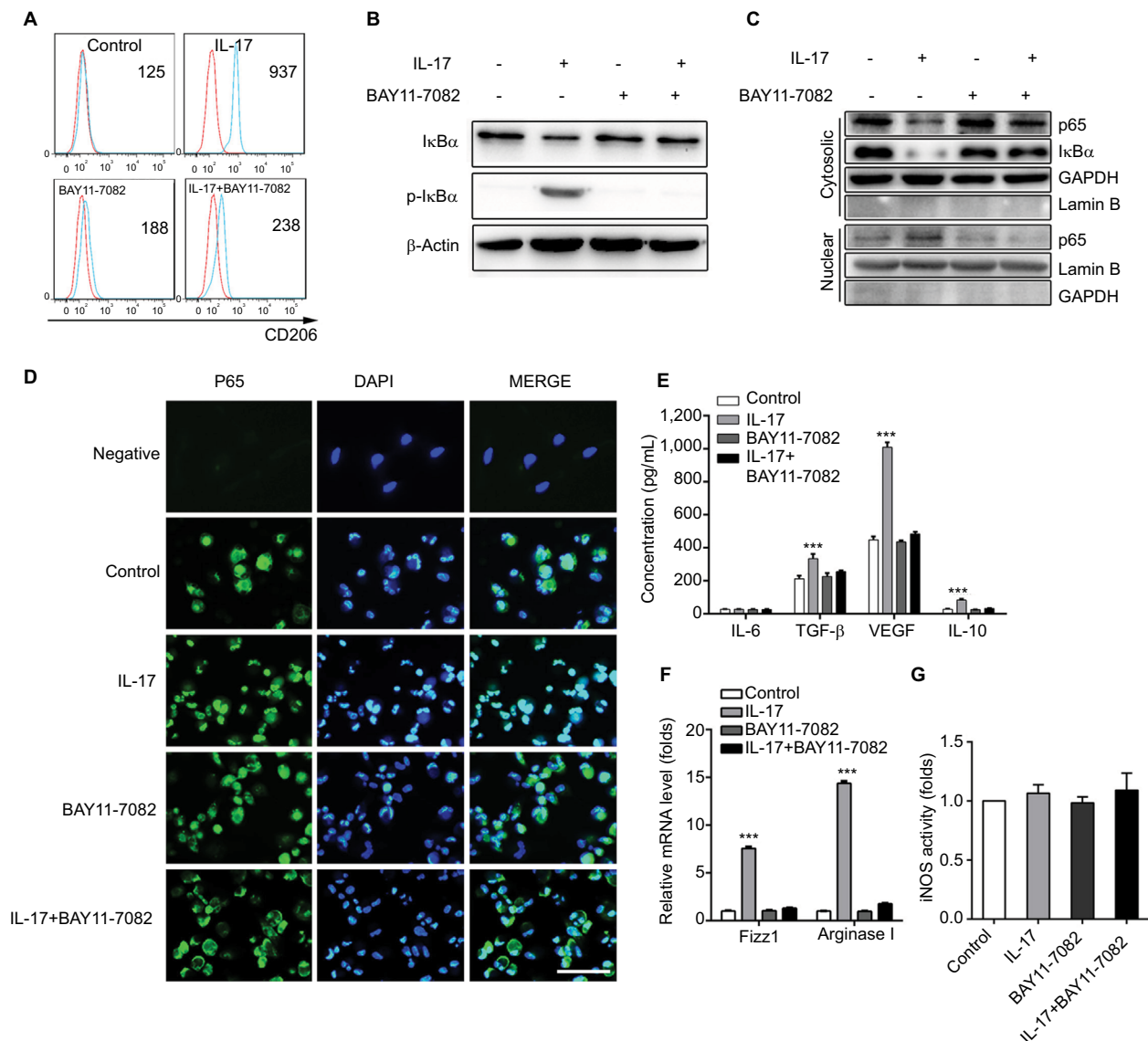


**Figure 2** IL-17 induces THP-1-derived macrophages to an M2-like phenotype via NF- $\kappa$ B.

**Notes:** (A) Flow cytometry analysis of CD206 expression in IL-17-treated and untreated THP-1-derived macrophages incubated in the presence or absence of NF- $\kappa$ B inhibitor BAY11-7082 for 48 hours. Numerical values denote the mean fluorescence intensity. The red line is the fluorescence intensity of isotype control. The blue line is the fluorescence intensity of CD206. (B) Immunoreactive bands for I $\kappa$ B $\alpha$  and p-I $\kappa$ B $\alpha$ . THP-1-derived macrophages were treated or untreated with IL-17 and NF- $\kappa$ B inhibitor BAY11-7082 for 48 hours. (C) Western blotting was utilized to determine the levels of p65, GAPDH and Lamin B in lysates from THP-1-derived macrophages. (D) Immunofluorescence assay of p65 expression and localization in THP-1-derived macrophages. Scale bar represents 0.05 mm. (E) ELISA analysis of cytokine levels in the media of THP-1-derived macrophages. The data shown represent mean $\pm$ SD (n=3 per group, \*\*\*P<0.001). (F) mRNA levels of Arginase I and Fizz1 were examined in THP-1-derived macrophages by real-time PCR. The data shown represent mean $\pm$ SD (n=3 per group, \*\*\*P<0.001). (G) iNOS activity was measured. The data shown represent mean $\pm$ SD (n=3 per group).

**Abbreviations:** DAPI, 40,6-diamidino-2-phenylindole; GAPDH, glyceraldehyde 3-phosphate dehydrogenase; h, hour; I $\kappa$ B $\alpha$ , nuclear factor kappa B inhibitor alpha; IL, interleukin; iNOS, inducible nitric oxide synthase; NF- $\kappa$ B, nuclear factor kappa B.

at 1, 2 and 5 years was 85.9%, 71.8% and 29.4%, respectively. Patients with high expression of IL-17 had poorer overall survival (OS) than those with low expression of IL-17 (Figure 5C). Similarly, there was an inverse correlation between intratumoral CD163+ cell or c-Maf+ cell density and patient survival (Figure 5D and E).

Univariate analysis revealed that intratumoral IL-17, CD163 and c-Maf expression were significantly associ-

ated with survival (Table 2). Patients were classified into the following four groups: group I, IL-17+ CD163+ c-Maf+; group II, IL-17-CD163-c-Maf-; group III, IL-17+ CD163-c-Maf- and group IV, IL-17+ CD163+ c-Maf- and IL-17+CD163-c-Maf+. Significant differences in survival were detected among group I and group II, but there was no statistical difference between group III and group IV (Figure 5F and G). Subsequently, in a multivariate COX

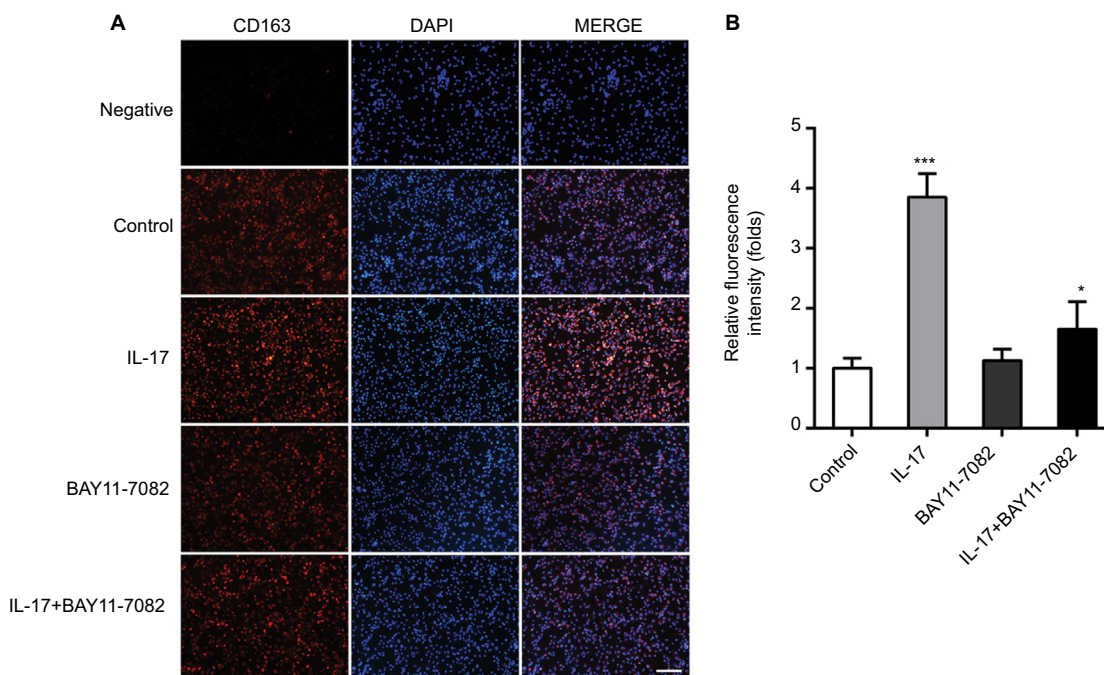


**Figure 3** BAY11-7082 inhibits IL-17-induced expression of CD163.

**Notes:** (A) Immunofluorescence assays showed that IL-17 (100 ng/mL for 48 hours) significantly elevated the expression of CD163 in THP-1-derived macrophages. However, the expression of CD163 was decreased if the NF- $\kappa$ B activity was blocked by BAY11-7082. Scale bar represents 0.1 mm. (B) Bar graph depicts the relative fluorescence intensity of CD163. The data shown represent mean $\pm$ SD (n=3 per group, \*P<0.05 and \*\*\*P<0.001).

**Abbreviations:** DAPI, 40,6-diamidino-2-phenylindole; IL, interleukin; NF- $\kappa$ B, nuclear factor kappa B.

**Table 2** Univariate and multivariate analyses of factors associated with survival

Variables	Univariate P-value	Multivariate	
		HR (95% CI)	P-value
Gender (female vs male)	NS	NA	NA
Age, years (<60 vs >60)	NS	NA	NA
Smoking status (smoker vs nonsmoker)	NS	NA	NA
TNM stage (I-II vs III-IV)	<0.001	2.252 (1.352–3.753)	0.002
Differentiation (well vs moderate-poor)	NS	NA	NA
Histological type (ADC vs non-ADC)	NS	NA	NA
IL-17 expression (low vs high)	0.023	NA	NS
CD163 expression (low vs high)	0.021	NA	NS
c-Maf expression (low vs high)	0.033	NA	NS
Combination of IL-17, CD163 and c-Maf			
IL-17+ CD163+ c-Maf+ vs IL-17-CD163-c-Maf-	0.03	1.394 (1.111–1.750)	0.004
IL-17+ CD163-c-Maf- vs IL-17+ CD163+/c-Maf+	NS	NA	NS

**Abbreviation:** ADC, adenocarcinomas; IL, interleukin; NS, not significant; NA, not assessed.

regression analysis where the presence of IL-17+ cells, CD163 expression, c-Maf expression and the combination of these markers were simultaneously adopted as covariates (Table 2), only the combination remained statistically significant, which was the comparison between groups I and II. These results collectively suggest that the combination of intratumoral IL-17+ cells, CD163 and c-Maf expression

serve as a better prognosis marker in NSCLC patients than either marker alone.

## Discussion

In this study, we show that IL-17 plays a potential role in promoting macrophages to a M2-like phenotype in a dose-dependent manner, which needs IL-17-persistent treatment.



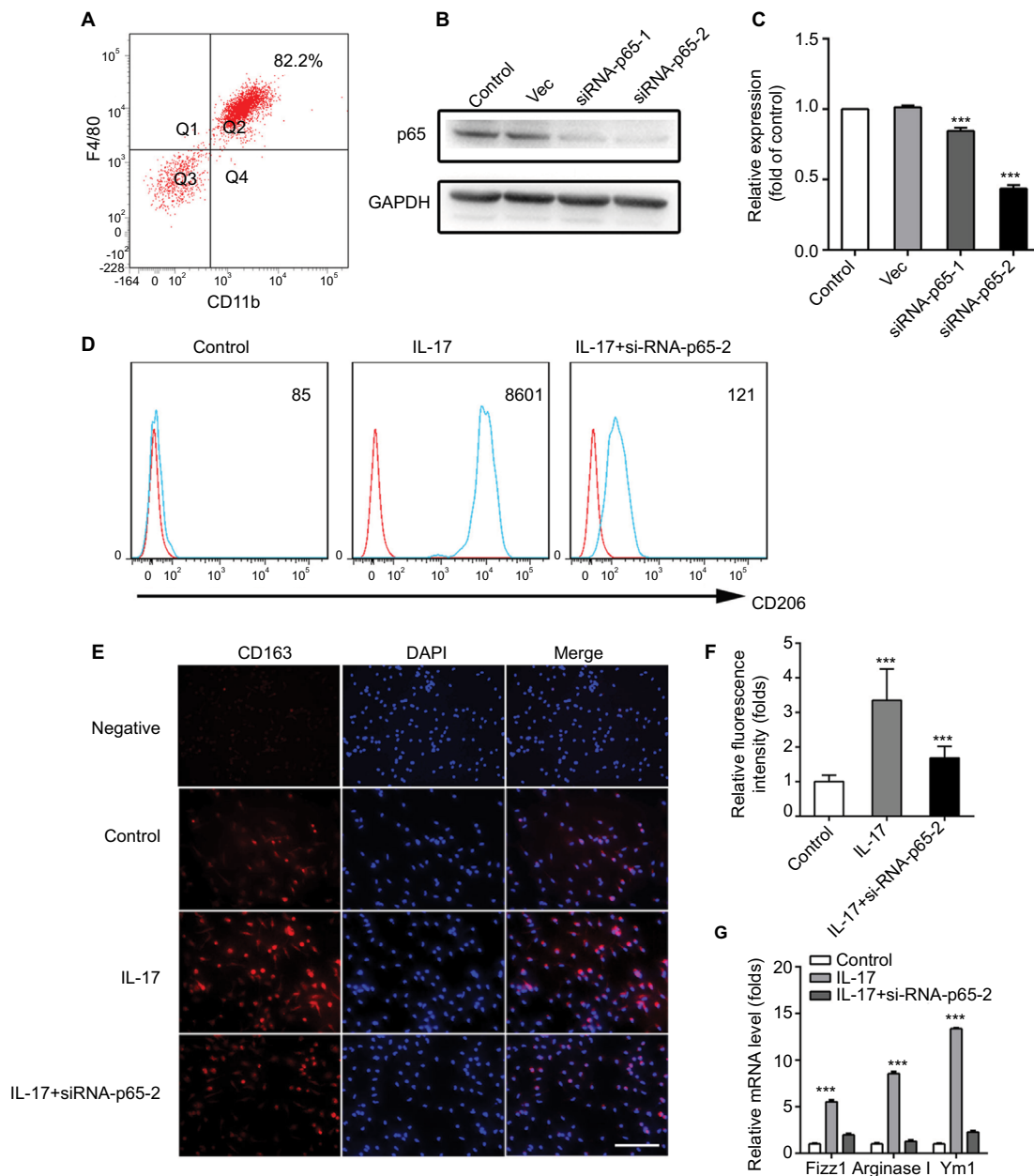


**Figure 4** IL-17 induces CD203 and CD163 expression in mouse peritoneal macrophages via p65.

**Notes:** (A) F4/80 and CD11b antibodies were used to authenticate by flow cytometry. (B and C) qRT-PCR and immunoreactive bands for p65 in mouse peritoneal macrophages treated with siRNA-p65. (D) Flow cytometry analysis of CD206 expression in IL-17-treated macrophages transfected with siRNA-p65. Numerical values denote the mean fluorescence intensity. The red line is the fluorescence intensity of isotype control. The blue line is the fluorescence intensity of CD206. (E) Immunofluorescence assay of CD163. Scale bar represents 0.1 mm. (F) Bar graph depicts the relative fluorescence intensity of CD163. The data shown represent mean $\pm$ SD (n=3 per group, \*\*\*P<0.001). (G) mRNA levels of Arginase I, Fizz1 and Ym1 were examined in mouse peritoneal macrophages by real-time PCR. The data shown represent mean $\pm$ SD (n=3 per group, \*\*\*P<0.001).

**Abbreviations:** DAPI, 40,6-diamidino-2-phenylindole; GAPDH, glyceraldehyde 3-phosphate dehydrogenase; IL, interleukin; qRT-PCR, quantitative real-time PCR; TGF- $\beta$ , transforming growth factor beta.

Additionally, NF- $\kappa$ B is involved in the IL-17-induced M2-like phenotype and high density of IL-17 and M2 macrophages are correlated with poor survival in NSCLC patients.

TAMs have been shown to promote tumor progression, and increased TAM infiltration often correlates with poor prognosis.<sup>22</sup> In previous study, TAMs are characterized as

mainly M2-like macrophages, which express a typical M2 marker profile including mannose receptor, a low MHC class II complex, stabilin-1 and Arginase I.<sup>3</sup> Cumulative evidence has highlighted a link between IL-17 and M2 polarization in several types of cancers.<sup>23</sup> We found that IL-17 treatment had a significant impact on M2 polarization, as evidenced

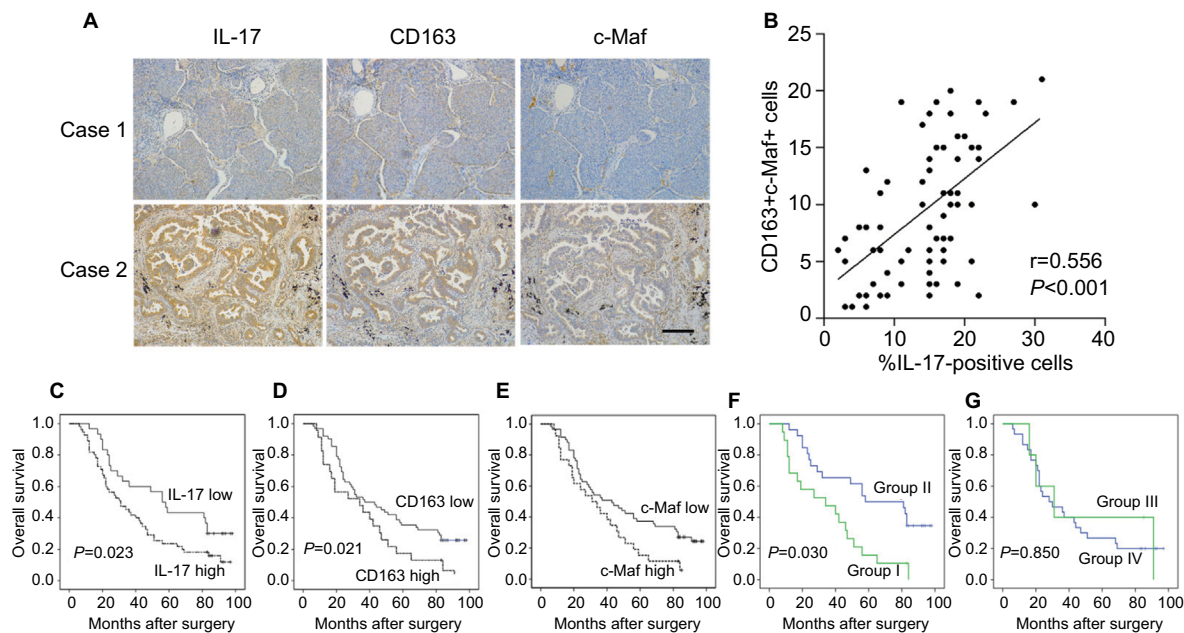


**Figure 5** CD163 and c-Maf expression positively correlates with IL-17+ cell and predicts poor survival of NSCLC patients.

**Notes:** (A) Serial whole tumor sections from 85 NSCLC patients were used, and representative cases of immunohistochemistry staining of IL-17, CD163 and c-Maf are shown (magnification, 200 $\times$ ). Scale bar represents 0.1 mm. (B) Significant positive correlations were found between the IL-17 expression and CD163+ c-Maf+ cells. (C–E) Kaplan–Meier curves of overall survival analysis between NSCLC patients. Patients with high expression of IL-17, CD163 and c-Maf had significantly poorer overall survival than patients with low expression. (F, and G) NSCLC patients were classified into the following four groups: group I, IL-17+ CD163+ c-Maf+; group II, IL-17-CD163-c-Maf-; group III, IL-17+ CD163-c-Maf- and group IV, IL-17+ CD163+ c-Maf- and IL-17+ CD163-c-Maf+. The survival rates in group I were significantly lower than those in group II. *P*-values were determined by the log-rank test.

**Abbreviations:** IL, interleukin; NSCLC, non-small-cell lung cancer.

by increased expression of M2 cell surface markers CD206 and CD163 in THP-1-derived macrophages and the mouse peritoneal macrophages. TAMs are often considered protumor due to secretion of growth- and angiogenesis-promoting factors.<sup>24</sup> These include the secretion of anti-inflammatory cytokines such as IL-10, CCL22 and TGF- $\beta$ , which can downmodulate macrophage ROS intermediates. Altogether, these factors suggest that enrichment of TAMs within the tumor microenvironment supports tumor growth and metastasis.<sup>25</sup> Consistent with our previous study, we found that IL-17 induced the higher levels of VEGF, which involved in angiogenesis promoting tumor metastasis.<sup>18</sup> Meanwhile, IL-10 and TGF- $\beta$  were increased after IL-17 treatment, which were anti-inflammatory cytokines in the tumor microenvironment supporting tumor growth.<sup>26</sup> Unlike findings from a previous study, our data suggest that the levels of IL-6 did not show significant change, this may due to the different types of cells.<sup>27</sup> Interestingly, after removing the stimulation of IL-17, the level of CD206 was gradually decreased. Our findings support the notion that IL-17 can promote M2-like phenotype in macrophages.

A number of downstream effectors can be activated by IL-17, the best studied member of this cytokine family, including the transcription factors NF- $\kappa$ B, C/EBP and AP-1, as well as MAP kinases.<sup>28</sup> NF- $\kappa$ B is an important transcription factor in regulating gene transcription. The activation of NF- $\kappa$ B was demonstrated by not only I $\kappa$ B $\alpha$  degradation and p65 translocation into the nucleus but also the binding of p65 to the targeted gene promoter.<sup>29</sup> A previous study showed that IL-17-induced epithelial–mesenchymal transition promoted lung cancer cell migration and invasion via the NF- $\kappa$ B signal pathway.<sup>16</sup> Combining all these reports, we sought to determine whether the NF- $\kappa$ B signaling pathway participates in the IL-17-induced M2-like phenotype. Our study showed that p-I $\kappa$ B $\alpha$  level and p65 nuclear translocation were increased in THP-1-derived macrophages treated with IL-17. When THP-1-derived macrophages were treated with the NF- $\kappa$ B inhibitor BAY11-7082, the increased p-I $\kappa$ B $\alpha$  level and p65 nuclear translocation induced by IL-17 were attenuated. In addition, the increased CD206 level was inhibited by siRNA-p65 in the mouse peritoneal macrophages. Thus, our results indicated that IL-17 activates the NF- $\kappa$ B

signaling pathway in macrophages. Arginase I, Ym1 and Fizz1 were secreted by M2 macrophages. The mRNA levels of Arginase I and Fizz1 in IL-17-treated THP-1-derived macrophages and Arginase I, Ym1 and Fizz1 in IL-17-treated mouse peritoneal macrophages were increased, which was abrogated by BAY 11-7082 and siRNA-p65-2, respectively. Based on these data, IL-17 induces macrophages to M2-like phenotype via NF-κB.

Tumor necrosis factor receptor-associated factor 3 (TRAF3) and interacting protein 2 (also known as Act1; CIKS) have been shown to be recruited to IL-17 receptor (IL-17R) through its SEF/IL-17R/CIKS/ACT1 homology (SEFIR) domain in an IL-17 stimulation-dependent manner.<sup>30</sup> Act1 was discovered to be essential for IL-17-induced activation of NF-κB. The inducible kinase IKKi (also named IKKe) was found to mediate the Act1-dependent and TRAF6-independent pathway. IKKi was shown to associate with Act1 in response to IL-17 treatment in mouse fibroblasts.<sup>31</sup> Thus, Act1 serves as a receptor proximal anchor platform for the initiation of NF-κB pathways activated by IL-17. In TNFα-mediated signaling, K63-linked TRAF6 polyubiquitination associates with the TAK1 complex and activates the kinase TAK1 and subsequently leads to the IKK complex and classic NF-κB activation.<sup>32</sup> The exact molecular mechanisms of IL-17 phosphorylating IκBα and activating NF-κB remain to be solved.

Recently, Xu et al have shown that lung cancer patients with pleural fluid IL-17 levels below 15 pg/mL had longer OS than those patients with higher levels (10.8 vs 4.7 months;  $P < 0.05$ ).<sup>33</sup> Consistent with these previous results, we found that IL-17 is associated with poor prognosis and that intratumoral IL-17-producing cells are positively correlated with CD163 and c-Maf in human NSCLC tissues. Barros et al reported that CD163 combination with c-Maf served to identify M2 macrophages better.<sup>34</sup> Although consistent with several recent publications regarding the role of IL-17 in promoting tumor progress, these findings contradict other reports, suggesting that IL-17 can provide an antitumor effect against certain tumors. Furthermore, the combination of intratumoral IL-17+ cells, CD163 and c-Maf expression served as a better predictor of poor survival than any alone in NSCLC patients.

## Acknowledgments

This work was supported by National Natural Science Foundation of China (81572824, 81773133 and 81701848), Natural Science Foundation of Heilongjiang Province (QC2016121, H2016051 and H2016047) and Innova-

tion Science Foundation of Harbin Medical University (2016LCZX57, 2016LCZX79 and 2017LCZX83). Jing Shen and Xin Sun are co-first authors.

## Disclosure

The authors report no conflicts of interest in this work.

## References

1. Declerck YA, Pienta KJ, Woodhouse EC, Singer DS, Mohla S. The Tumor Microenvironment at a Turning Point Knowledge Gained Over the Last Decade, and Challenges and Opportunities Ahead: A White Paper from the NCI TME Network. *Cancer Res.* 2017;77(5):1051–1059.
2. Condeelis J, Pollard JW. Macrophages: obligate partners for tumor cell migration, invasion, and metastasis. *Cell.* 2006;124(2):263–266.
3. Mantovani A, Sozzani S, Locati M, Allavena P, Sica A. Macrophage polarization: tumor-associated macrophages as a paradigm for polarized M2 mononuclear phagocytes. *Trends Immunol.* 2002;23(11):549–555.
4. Mantovani A, Sica A. Macrophages, innate immunity and cancer: balance, tolerance, and diversity. *Curr Opin Immunol.* 2010;22(2):231–237.
5. Siveen KS, Kuttan G. Role of macrophages in tumour progression. *Immunol Lett.* 2009;123(2):97–102.
6. Gordon S, Martinez FO. Alternative activation of macrophages: mechanism and functions. *Immunity.* 2010;32(5):593–604.
7. Prokop S, Heppner FL, Goebel HH, Stenzel W. M2 polarized macrophages and giant cells contribute to myofibrosis in neuromuscular sarcoidosis. *Am J Pathol.* 2011;178(3):1279–1286.
8. Chen Z, Feng X, Herting CJ, et al. Cellular and Molecular Identity of Tumor-Associated Macrophages in Glioblastoma. *Cancer Res.* 2017;77(9):2266–2278.
9. Chanmee T, Ontong P, Konno K, Itano N. Tumor-associated macrophages as major players in the tumor microenvironment. *Cancers.* 2014;6(3):1670–1690.
10. Wang R, Zhang J, Chen S, et al. Tumor-associated macrophages provide a suitable microenvironment for non-small lung cancer invasion and progression. *Lung Cancer.* 2011;74(2):188–196.
11. Chen C, Itakura E, Nelson GM, et al. IL-17 is a neuromodulator of *Caenorhabditis elegans* sensory responses. *Nature.* 2017;542(7639):43–48.
12. Song X, Qian Y. The activation and regulation of IL-17 receptor mediated signaling. *Cytokine.* 2013;62(2):175–182.
13. Ha HL, Wang H, Pisitkun P, et al. IL-17 drives psoriatic inflammation via distinct, target cell-specific mechanisms. *Proc Natl Acad Sci U S A.* 2014;111(33):E3422–3431.
14. Mehrotra P, Collett JA, Mckinney SD, et al. IL-17 mediates neutrophil infiltration and renal fibrosis following recovery from ischemia reperfusion: compensatory role of natural killer cells in athymic rats. *Am J Physiol Renal Physiol.* 2017;312(3):F385–F397.
15. Zhang Q, Atsuta I, Liu S, et al. IL-17-mediated M1/M2 macrophage alteration contributes to pathogenesis of bisphosphonate-related osteonecrosis of the jaws. *Clin Cancer Res.* 2013;19(12):3176–3188.
16. Gu K, Li MM, Shen J, et al. Interleukin-17-induced EMT promotes lung cancer cell migration and invasion via NF-κB/ZEB1 signal pathway. *Am J Cancer Res.* 2015;5(3):1169–1179.
17. Li Q, Liu L, Zhang Q, et al. Interleukin-17 Indirectly Promotes M2 Macrophage Differentiation through Stimulation of COX-2/PGE2 Pathway in the Cancer Cells. *Cancer Res Treat.* 2014;46(3):297–306.
18. Pan B, Shen J, Cao J, et al. Interleukin-17 promotes angiogenesis by stimulating VEGF production of cancer cells via the STAT3/GIV signaling pathway in non-small-cell lung cancer. *Sci Rep.* 2015;5:16053.
19. Quatromoni JG, Eruslanov E. Function Tumor-Associated Macrophages: phenotype, and link to prognosis in human lung cancer. *Am J Transl Res.* 2012;4(4):376–389.

20. Lin D, Li L, Sun Y, et al. IL-17 regulates the expressions of RANKL and OPG in human periodontal ligament cells via TRAF6/TBK1-JNK/NF- $\kappa$ B pathways. *Immunology*. 2015;144(3):472–485.
21. Chen XW, Zhou S-F. Inflammation, cytokines, the IL-17/IL-6/STAT3/NF- $\kappa$ B axis, and tumorigenesis. *Drug Des Devel Ther*. 2015;9:2941–2946.
22. Chen G. The relationship between the expression of TAM, survivin and the degree of necrosis of the tumor after cisplatin treatment in osteosarcoma. *Eur Rev Med Pharmacol Sci*. 2017;21(3):490–497.
23. Nishikawa K, Seo N, Torii M, et al. Interleukin-17 induces an atypical M2-like macrophage subpopulation that regulates intestinal inflammation. *PLoS One*. 2014;9(9):e108494.
24. Mantovani A, Locati M. Tumor-associated macrophages as a paradigm of macrophage plasticity, diversity, and polarization: lessons and open questions. *Arterioscler Thromb Vasc Biol*. 2013;33(7):1478–1483.
25. Ruffell B, Affara NI, Coussens LM. Differential macrophage programming in the tumor microenvironment. *Trends Immunol*. 2012;33(3):119–126.
26. Rahmah Z, Sasmito SD, Siswanto B, Sardjono TW, Fitri LE. Parasitemia Induces High Plasma Levels of Interleukin-17 (IL-17) and Low Levels of Interleukin-10 (IL-10) and Transforming Growth Factor- $\beta$  (TGF- $\beta$ ) in Pregnant Mice Infected with Malaria. *Malays J Med Sci*. 2015;22(3):25–32.
27. Kimura A, Naka T, Kishimoto T. IL-6-dependent and -independent pathways in the development of interleukin 17-producing T helper cells. *Proc Natl Acad Sci U S A*. 2007;104(29):12099–12104.
28. Gaffen SL. Structure and signalling in the IL-17 receptor family. *Nat Rev Immunol*. 2009;9(8):556–567.
29. Shu G, Zhang L, Jiang S, et al. Isoliensinine induces dephosphorylation of NF- $\kappa$ B p65 subunit at Ser536 via a PP2A-dependent mechanism in hepatocellular carcinoma cells: roles of impairing PP2A/I2PP2A interaction. *Oncotarget*. 2016;7(26):40285–40296.
30. Onishi RM, Park SJ, Hanel W, et al. SEF/IL-17R (SEFIR) is not enough: an extended SEFIR domain is required for il-17RA-mediated signal transduction. *J Biol Chem*. 2010;285(43):32751–32759.
31. Sønder SU, Saret S, Tang W, et al. IL-17-induced NF- $\kappa$ B activation via CIKS/Act1: physiologic significance and signaling mechanisms. *J Biol Chem*. 2011;286(15):12881–12890.
32. Chen ZJ. Ubiquitin signalling in the NF- $\kappa$ B pathway. *Nat Cell Biol*. 2005;7(8):758–765.
33. Xu C, Yu L, Zhan P, Zhang Y. Elevated pleural effusion IL-17 is a diagnostic marker and outcome predictor in lung cancer patients. *Eur J Med Res*. 2014;19:23.
34. Barros MH, Hauck F, Dreyer JH, Kempkes B, Niedobitek G. Macrophage polarisation: an immunohistochemical approach for identifying M1 and M2 macrophages. *PLoS One*. 2013;8(11):e80908.

## Cancer Management and Research

### Publish your work in this journal

Cancer Management and Research is an international, peer-reviewed open access journal focusing on cancer research and the optimal use of preventative and integrated treatment interventions to achieve improved outcomes, enhanced survival and quality of life for the cancer patient. The manuscript management system is completely online and includes

a very quick and fair peer-review system, which is all easy to use. Visit <http://www.dovepress.com/testimonials.php> to read real quotes from published authors.

Submit your manuscript here: <https://www.dovepress.com/cancer-management-and-research-journal>

Dovepress